

Collision quenching of the metastable 2S state of muonic hydrogen and the muonic helium ion*

R. O. Mueller, V. W. Hughes, and H. Rosenthal†

Gibbs Laboratory, Yale University, New Haven, Connecticut 06520

C. S. Wu

Physics Department, Columbia University, New York, New York 10027

(Received 22 July 1974)

We present calculations of the cross section for quenching of the metastable 2S state of muonic hydrogen (μ^-p) in collisions with a hydrogen atom, at collision energies below the threshold for inelastic 2S-2P excitation. A quantum mechanical approach based on the adiabatic approximation is used with phase shifts evaluated in the WKB approximation. Below threshold, the dominant quenching process involves Stark admixture of 2S and 2P states of μ^-p during the collision, which is accompanied by a 2P-1S radiative transition also during the collision, and consequently the cross section is reduced by several orders of magnitude compared with the inelastic cross section. These results are important to considerations of the possibility of measuring the $n = 2$ fine and hyperfine structures of μ^-p . We also present quenching cross section results based on this same approach for collisions of the muonic helium ion, $(\mu^- \alpha)^+$, on He, relevant to lifetime and fine-structure measurements of $(\mu^- \alpha)^+$. Our theoretical results for $(\mu^- \alpha)^+$ differ from available experimental lifetime results for $(\mu^- \alpha)^+$. We attribute the discrepancy to uncertainties in the values of the interatomic potential used in the calculations.

I. INTRODUCTION

Precise measurement of the fine-structure and hyperfine-structure energy levels of muonic hydrogen (μ^-p) would be of great value to the topics of muon electrodynamics and proton structure.¹⁻³ The energy-level scheme of the ground $n = 1$ and first excited $n = 2$ states of μ^-p is shown in Fig. 1. Because of a much larger electron vacuum-polarization contribution to the 2S level than to the 2P levels, the 2S level is shifted below the 2P levels; precise measurement of the 2^2P-2^2S energy difference would provide a sensitive test of electron vacuum polarization.³ Also, the contributions of proton structure and relativistic recoil to the 2S state hyperfine structure interval are relatively large.

A measurement has been reported^{4,5} on the $2^2P_{3/2}-2^2S_{1/2}$ Lamb shift of the muonic helium ion $(\mu^- \alpha)^+$, which is also of great value as a test of vacuum polarization.⁶ For simplicity, we denote $(\mu^- \alpha)^+$ as $\mu^- \alpha$. The method involves forming $\mu^- \alpha$ ions in the 2S state by stopping negative muons in helium gas, inducing electric dipole transitions with a laser light source from a 2S level to a 2P level, and observing the resonant enhancement in the time distribution of 2P-1S x rays for $\mu^- \alpha$. The method relies on the metastability of the $\mu^- \alpha(2S)$ ions within the helium gas environment.

In considering an analogous experiment for μ^-p it is crucial to know the number of metastable 2S atoms that can be formed, and how rapidly atomic collision-quenching processes deplete these μ^-p

(2S) atoms. We will be concerned here solely with the lifetime problem of $\mu^-p(2S)$ and $\mu^- \alpha(2S)$.

For free $\mu^-p(2S)$ the dominant decay mode is⁴ simply muon decay with a decay rate of $4.5 \times 10^5 \text{ sec}^{-1}$. The two-photon radiative transition to the 1S state^{4,7} has a rate of $1.7 \times 10^3 \text{ sec}^{-1}$, and hence the small branching ratio of 3.8×10^{-3} . The rate of muon capture by the proton is much smaller. For $\mu^- \alpha(2S)$ the two-photon decay is $1.1 \times 10^5 \text{ sec}^{-1}$.

Stability of $\mu^-p(2S)$ in H_2 gas with respect to collision quenching to the 1S state depends critically upon whether the relative kinetic energy is less than or greater than the magnitude of the 2P-2S energy separation ν_L of μ^-p , where $\nu_L = 0.2 \text{ eV}$. In the laboratory frame this inelastic threshold is about 0.31 eV in a collision with a stationary H_2 molecule. The precise kinetic-energy distribution of $\mu^-p(2S)$ after formation, as well as the probability that a 2S state is formed, depend on a large number of atomic and molecular processes, including chemical reactions, involved in the slowing down of μ^- in the H_2 gas⁸ and in the formation of the 2S state.^{9-11,4} As a result of the possibility of chemical reactions it has been pointed out¹⁰ that μ^-p can in principle acquire kinetic energies in the eV range during the de-excitation process. Indeed, the kinetic-energy distribution of $\mu^-p(2S)$, or simply the number of atoms with kinetic energies above and below the inelastic threshold, depends on too many complicated processes to calculate reliably. Furthermore, experimental evidence on

this distribution available from a diffusion-type experiment¹² is not sufficiently quantitative.

If the relative kinetic energy of the collision is greater than ν_L , inelastic excitations involving $2S \rightarrow 2P$ transitions can occur. The atom will then radiate¹³ to the $1S$ state, so its metastability is quenched by the collision. The radiative decay $2P \rightarrow 2S$ is, of course, totally negligible in comparison with the decay to the $1S$ state. Collision times are quite short in comparison with the radiative lifetime τ_R ; therefore radiation to the $1S$ state will predominantly occur after the collision. At a relative kinetic energy of 1 eV for example, the relative velocity is about 2×10^6 cm/sec, and the transit time τ_c over a region of several Bohr radii is about 10^{-14} sec, which is considerably shorter than the radiative lifetime τ_R of the $2P$ state where $\tau_R = 0.8 \times 10^{-11}$ sec. The cross section for this process has been previously calculated¹⁴ using an inelastic straight-line impact-parameter approach, and is about 10^{-16} cm² at a relative kinetic energy of 1 eV. Further, it is not particularly sensitive to the value of the relative kinetic energy above the inelastic threshold. At pressures useful for stopping muons, even as low as one atmosphere, this value of the quenching cross section corresponds¹⁵ to depletion rates as high as 10^{10} sec⁻¹; such a high depletion rate makes a spectroscopy experiment on the $n=2$ state extremely difficult.

If the relative kinetic energy is below the threshold ν_L , this inelastic process is energetically forbidden. Quenching will still occur, however, through a physical process that involves Stark admixture of the $2S$ and $2P$ states during the collision, with an electric dipole transition to the $1S$ state also taking place during the collision.¹⁶ Since in this process the radiative transition to the $1S$ state must occur during the collision, we would, in order of magnitude, expect the corresponding cross section to be reduced by the factor (τ_c/τ_R) relative to the inelastic cross section, leading to a cross-section value of order 10^{-19} cm². At one atmosphere pressure of H₂ gas, $\mu^-p(2S)$ would have a lifetime against collision quenching about equal to the free-muon lifetime. Hence, provided a reasonable fraction of the μ^-p atoms have kinetic energies less than ν_L , this situation would make it reasonable to consider a fine-structure measurement on μ^-p , using the very-high-intensity muon beams becoming available at the new meson factories.

In this paper we present detailed calculations of this so-called Stark-mixing quenching cross section applicable at relatively low collision energies of μ^-p on H₂, based on the adiabatic approximation in which all inelastic excitations are neglected. Calculations are carried out with both a semiclassical impact-parameter approach and a quantum-

mechanical partial-wave analysis of the relative motion, with phase shifts computed in the WKB approximation.

We also present results for the collision-quenching cross section below threshold for $\mu^- \alpha$ on He, relevant to lifetime and fine structure measurements on $\mu^- \alpha(2S)$. In the slowing down of μ^- in helium gas and formation of $\mu^- \alpha(2S)$ ions, chemical reactions are not believed important and hence it is expected that $\mu^- \alpha$ will have the thermal kinetic energies of the He atoms. Since the $2P-2S$ energy separation of $\mu^- \alpha$ is about 1.4 eV, inelastic collisions $2S-2P$ are not energetically possible.

The arrangement of the paper is as follows. In Sec. II we derive approximate interatomic potential-energy curves. In Sec. III the validity of the adiabatic approximation is briefly discussed. In Secs. IV and V we present the quantum-mechanical and impact-parameter calculations, respectively. Section VI is a final discussion.

II. INTERATOMIC POTENTIAL-ENERGY CURVES

Calculation of the relevant interatomic potential-energy curves for $\mu^-p(2S)$ on H₂ simplifies in lowest order because of the properties of $\mu^-p(2S)$. Firstly, since μ^-p is small and neutral, it does not affect, in lowest order, the electronic structure of an atom it collides with; $\mu^-p(2S)$ does become polarized but because of the smallness of the induced electric dipole moment its effect on

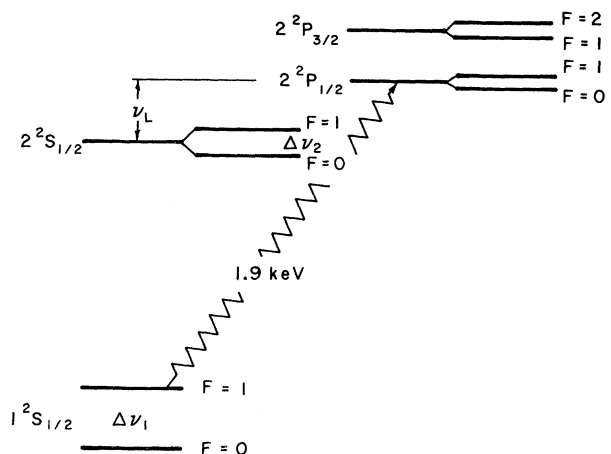


FIG. 1. Schematic diagram of the energy levels of muonic hydrogen (μ^-p) in the $n=1$ and $n=2$ states. The $2^2S_{1/2}-2^2P_{1/2}$ interval ν_L is 0.2 eV, the $2^2P_{1/2}-2^2P_{3/2}$ fine structure interval is 0.008 eV and the hyperfine structure interval in the ground state $\Delta\nu_1$ is 0.2 eV.

the electronic structure of the other atom may be neglected, even when it is "well inside" this atom.

Secondly, the perturbation of the $\mu^-p(2S)$ atom, as it passes the target atom and is subject to the electric fields of the target atom, remains totally negligible relative to the magnitude of the energy separation of the low principal-quantum-number states of μ^-p . Significant mixing occurs only in the subspace of "nearly degenerate" $n=2$ states through a linear Stark effect and, because of the magnitude of the $2S-2P$ energy separation, only if μ^-p is within the target atom. Thus, the electric field strength of the unscreened proton at a_0 is $e/a_0^2 \approx 5 \times 10^9$ v/cm, which leads to a first-order Stark energy for $\mu^-p(2S)$ of only 1 eV whereas the corresponding $2S-1S$ energy separation is 1.9 keV. The perturbation on the $\mu^-p(2S)$ atom is most significant when it is close to one of the protons in H_2 and hence to a good approximation, the H_2 molecule can be treated as two independent H atoms. We now consider the much simpler collision problem of μ^-p on a hydrogen atom.

Further, since ν_L is more than an order of magnitude larger than the fine structure $2^3P_{3/2}-2^2P_{1/2}$ and still larger than hyperfine structure in μ^-p , the effect of the muon's spin can be neglected and the $n=2$ states are described in terms of simple nonrelativistic hydrogen-like orbitals with the energy of the $2S$ state depressed by ν_L relative to the degenerate $2P$ states.

The coordinate system used for collisions of $\mu^-p(2S)$ on H is shown in Fig. 2. The interatomic position vector \vec{R} connects the proton in H with the center of mass (c.m.) of μ^-p . With this coordinate system, nonadiabatic coupling terms involving the muon's coordinate will vanish asymptotically. The position coordinates \vec{r}_μ and \vec{r} of the muon and electron are expressed relative to their respective nuclei; separated atom coordinates are appropriate to use since the interatomic interaction is treated as a perturbation at all values of $R = |\vec{R}|$. With these coordinates, the total kinetic energy separates approximately into the kinetic energy of the over-all c.m., the kinetic energy of the relative interatomic motion, and the internal kinetic energies of the atoms. Small cross terms on the order of the electron-to-proton mass are neglected.

Since the range of relative interatomic velocities

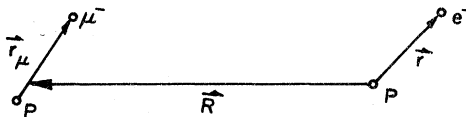


FIG. 2. Coordinate system used for collisions of μ^-p on H. Analogous coordinates are used for $(\mu^-a)^+$ on He.

of interest is so low compared with electron and muon bound-state velocities, which are of order $Z\alpha c/n$, a conventional Born-Oppenheimer approximation is applied. For fixed R , the effective Schrödinger equation for the wave function describing the electron and muon motion is written

$$\mathcal{H}\Psi(\vec{r}_\mu, \vec{r}; \vec{R}) = [H_0(\vec{r}) + H(\vec{r}_\mu) + V(\vec{r}_\mu, \vec{r}; \vec{R})]\Psi(\vec{r}_\mu, \vec{r}; \vec{R}) = E\Psi, \quad (2.1)$$

where H_0 is the nonrelativistic internal Hamiltonian for the hydrogen atom, H is the internal Hamiltonian for μ^-p including terms for the Lamb-shift separation and radiative decay of the $2P$ state (as detailed below), V comprises the Coulomb interactions between the atoms including mutual nuclear repulsion, and \vec{R} appears only parametrically in V and Ψ .

In line with the above discussion, Ψ is taken in lowest order to be a direct product of a $1S$ hydrogenic function for the H atom with a linear combination of $2S$ and $2P$ hydrogen-like orbitals for μ^-p , which accounts for near resonance of its $n=2$ internal states. This form, which in most collisions is only valid asymptotically, is assumed valid in the present case at all separations R . The correct zeroth-order linear combination of $2S$ and $2P$ orbitals for the μ^-p wave functions is then determined by diagonalization of the Hamiltonian \mathcal{H} , and depends on \vec{R} . We note that the direct product form for Ψ is valid since there is no over-all symmetry requirement. The only dependence of Ψ on \vec{R} is in the wave function for μ^-p .

Multiplication by the $1S$ hydrogenic wave function of the H atom on the right and left of the Hamiltonian \mathcal{H} , and integration over the electron's coordinates leads to the effective Hamiltonian for the internal motion of μ^-p

$$H_{\text{eff}}(\vec{r}_\mu; \vec{R}) = E_H + H(\vec{r}_\mu) - eV_{1S}[|\vec{R} + (m_p/M)\vec{r}_\mu|] + eV_{1S}[|\vec{R} - (m_\mu/M)\vec{r}_\mu|], \quad (2.2)$$

where m_p and m_μ are the proton and muon masses, M is total mass of μ^-p , E_H is the energy of the H atom [$E_H = -e^2/(2a_0) = -13.6$ eV], and V_{1S} is the spherically symmetric Coulomb potential generated by the H atom. For the important region $|r_\mu| < R$ the potential terms vary only slightly over the dimensions of μ^-p , and are expanded about R ; the first nonvanishing contribution from the sum of the potential terms is $e\vec{E}(R) \cdot \vec{r}_\mu$, where $\vec{E}(R)$ is the radial, outward directed, electric field of the H atom with magnitude

$$|\vec{E}(R)| = R^{-2}(1 + 2R + 2R^2)e^{-2R}(e/a_0^2), \quad (2.3)$$

where R is in units of a_0 .

The internal states of μ^-p are assumed quantized relative to the body-fixed \vec{R} axis. Since the electric

field is also along \vec{R} , the Stark effect in lowest order mixes the $2S$ state only with the $2P$ state of projection $m_l = 0$; the $2P$ states of projection $m_l = \pm 1$ remain unaffected to lowest order, and are not included in the description given below of the diagonalization of H_{eff} in the $n = 2$ subspace.

The matrix elements of H_{eff} with the asymptotic basis functions, ϕ_{2S} and $\phi_{2P}^0(m_l = 0)$, are then

$$\langle H_{\text{eff}} \rangle = \begin{pmatrix} \langle \phi_{2S}, H_{\text{eff}} \phi_{2S} \rangle & \langle \phi_{2S}, H_{\text{eff}} \phi_{2P}^0 \rangle \\ \langle \phi_{2P}^0, H_{\text{eff}} \phi_{2S} \rangle & \langle \phi_{2P}^0, H_{\text{eff}} \phi_{2P}^0 \rangle \end{pmatrix} = \begin{pmatrix} -\Delta & c \\ c & \Delta - i\gamma/2 \end{pmatrix}, \quad (2.4)$$

where $2\Delta (= \nu_L)$ is the Lamb shift of $2S$ and $2P$ states, $\gamma \equiv \hbar/\tau_R$ is the radiative width of the $2P$ state, and all constant energy terms have been absorbed in the energy zero point which is now taken at the midpoint of the $2S$ and $2P$ levels. Radiative decay of the $2P$ state is accounted for in the usual phenomenological fashion with an imaginary Hamiltonian term which projects only on the $2P$ state, $H_{\text{decay}} = (-i\gamma/2) |\phi_{2P}^0\rangle \langle \phi_{2P}^0|$. c is the first-order Stark energy,

$$c = (\phi_{2S}, e\vec{E}(R) \cdot \vec{r}_\mu \phi_{2P}^0) = 3e(a_\mu/Z) |\vec{E}(R)|, \quad (2.5)$$

where if the reduced mass of μ^-p is denoted m_μ^* , then $a_\mu \equiv \hbar^2/m_\mu^*e^2$ is the Bohr radius for μ^-p .

Since H_{decay} is a small term relative to Δ , $\langle H_{\text{eff}} \rangle$ is diagonalized with H_{decay} neglected leading to the following zeroth-order linear combinations of ϕ_{2S} and ϕ_{2P}^0 orbitals

$$\Psi_{2S}(\vec{r}_\mu; R) = A(R)\phi_{2S}(\vec{r}_\mu) + B(R)\phi_{2P}^0(\vec{r}_\mu), \quad (2.5a)$$

$$\Psi_{2P}^0(\vec{r}_\mu; R) = -B(R)\phi_{2S}(\vec{r}_\mu) + A(R)\phi_{2P}^0(\vec{r}_\mu), \quad (2.5b)$$

with corresponding first-order energies

$$\epsilon_{2S} = -\epsilon(R), \quad (2.6a)$$

$$\epsilon_{2P}^0 = +\epsilon(R), \quad (2.6b)$$

where

$$\epsilon(R) \equiv [\Delta^2 + c^2(R)]^{1/2}. \quad (2.7)$$

The real amplitudes satisfying unitarity ($A^2 + B^2 = 1$), are

$$A(R) = c(R) \left(\frac{1}{2\epsilon(R)[\epsilon(R) - \Delta]} \right)^{1/2} \quad (2.8)$$

$$B(R) = - \left(\frac{\epsilon(R) - \Delta}{2\epsilon(R)} \right)^{1/2}.$$

The energies ϵ_{2S} and ϵ_{2P}^0 are shown in Fig. 3. (Also included are the energies $\epsilon_{2P}^{\pm 1} = \Delta$ for the $2P$ states

of projections $m_l = \pm 1$, which are unperturbed to lowest order.) The states Ψ_{2S} and Ψ_{2P}^0 are orthonormal for all R and represent the lowest-order $m_l = 0$ adiabatic solutions; they are denoted by the $2S$ and $2P(m_l = 0)$ asymptotic orbitals which they reduce to for $R \rightarrow \infty$.

H_{decay} is not diagonal in the adiabatic basis,

$$\langle H_{\text{decay}} \rangle = \frac{-i\gamma}{2} \begin{pmatrix} B^2 & AB \\ AB & A^2 \end{pmatrix}. \quad (2.9)$$

Since it is small, however, it is evaluated to first order with the nondegenerate adiabatic states, which leads to the addition of the diagonal terms in (2.9) to the energies (2.6). The $m_l = 0$ adiabatic interatomic potential curves, which are now slightly complex and which are defined relative to the asymptotic internal energies of the colliding atoms so as to fall to zero at $R \rightarrow \infty$, are then

$$\nu_{2S}(R) = -\epsilon(R) + \Delta - \frac{1}{2}i\gamma B^2(R), \quad (2.10a)$$

$$\nu_{2P}^0(R) = \epsilon(R) - \Delta - \frac{1}{2}i\gamma A^2(R). \quad (2.10b)$$

The imaginary terms, corresponding to the opacity of the optical potentials, are proportional to the decay rate of the $2P$ state and the amplitude squared of the $2P$ -state component in each of the adiabatic solutions. $B^2(R)$ is shown in Fig. 4 [$A^2(R) = 1 - B^2(R)$]; it attains the value $\frac{1}{2}$ at $R \rightarrow 0$ where $|\vec{E}(R)|$ and hence $\epsilon(R)$ are infinite, although this perturbative approach breaks down well before this limit is reached.

A similar approach is used for collisions of $\mu^- \alpha$ on He. However, since $\mu^- \alpha$ is positively charged it affects the electronic structure of the target atom. To lowest order, it is assumed to affect the He atom, which is in its ground state, in

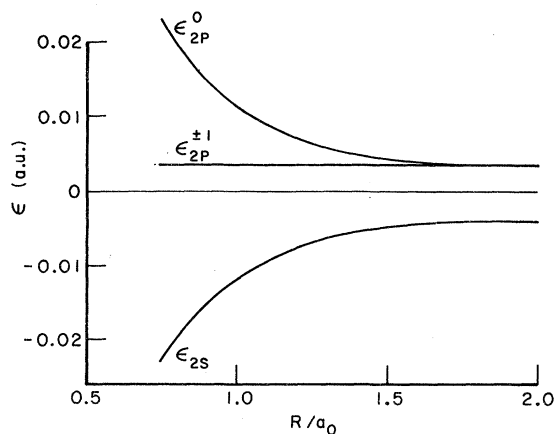


FIG. 3. Energy levels, including the Lamb shift and first-order Stark corrections, of the different $n = 2$ states of μ^-p as a function of the separation R of μ^-p from H. The energy zero point is chosen at the midpoint of the asymptotic ($R \rightarrow \infty$) separation of the levels.

the same way as an incident proton. (The difference in mass plays no role with regard to solution of the electronic motion.) For fixed \vec{R} , the wave function for motion of electrons and muons is then taken in lowest order to be a product of the ground-state electronic wave function describing a helium atom in the presence of a proton at position \vec{R} with a linear combination of hydrogen-like 2S and 2P orbitals for $\mu^- \alpha$. With reference to the electronic motion, approximate variational calculations of the $X^1\Sigma^+$ ground-state energy of the system $(\text{HeH})^+$ have been carried out¹⁷ over a limited range of separations R , and in Fig. 5 we depict the form of the interatomic potential-energy curve, which we denote by $V'(R)$. The minimum in the curve has a depth of about 2.0 eV at the equilibrium separation, $R_e = 1.46a_0$. An approximate Morse fit to this potential curve, which matches quite closely the numerical values¹⁷ available in the range $1.1 < R < 1.8$, is

$$V'(R) \simeq -0.075[1 - (1 - e^{-1.65(R-1.46)})^2](e^2/a_0), \quad (2.11)$$

where R is in units of a_0 . Although the Morse fit is incorrect asymptotically since it falls off exponentially rather than as R^{-4} , corresponding to the charge induced dipole interaction of $(\text{HeH})^+$, this is unimportant to the quenching process which occurs predominantly at small separations R . Since the accuracy of the numerical results for V' in Ref. 17 is not known, and since a Morse extrapolation is used to reach sufficiently small values of R , the quenching results are quite uncertain in this case and suggest the need for precise determination of V' over a larger range of separations.

By the same approach as before, we obtain the following effective Hamiltonian for the internal motion of $\mu^- \alpha$,

$$H_{\text{eff}}(\vec{r}_\mu; \vec{R}) = E_{\text{He}}^0 + H(\vec{r}_\mu) + V'(R) - ev'(\vec{R}) - ev'[\vec{R} + (m_\alpha/M)\vec{r}_\mu] + 2ev'[\vec{R} - (m_\mu/M)\vec{r}_\mu], \quad (2.12)$$

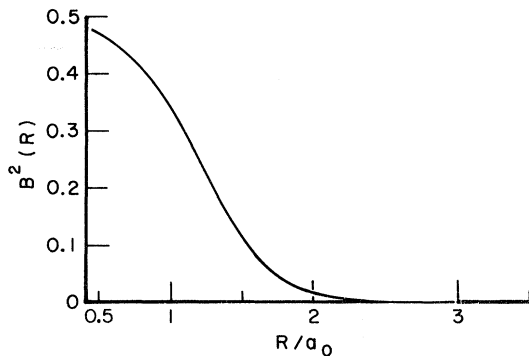


FIG. 4. $B^2(R)$ vs R for $\mu^- p$ on H.

where E_{He}^0 is the ground-state energy of He at infinite separation from $\mu^- \alpha$, symbols used previously are defined in an obvious analogous fashion for $\mu^- \alpha$, and $v'(\vec{X})$ is the electrostatic potential at position \vec{X} generated by the He atom, including its nucleus in the presence of the proton at \vec{R} . v' is not, of course, spherically symmetric. As before, we expand the potential terms about \vec{R} , and the first nonvanishing contribution is $e(1 + m_\mu/M) \times \vec{E}(\vec{R}) \cdot \vec{r}_\mu$, where $\vec{E}(\vec{R}) = -\partial v'(\vec{R})/\partial \vec{R}$. The small factor m_μ/M is neglected. From symmetry, \vec{E} , at points along the \vec{R} axis, is radially directed. Assuming the applicability of the Hellmann-Feynman theorem¹⁸ (see the final comment of this section), the magnitude of \vec{E} along the \vec{R} axis is given simply by

$$|\vec{E}(\vec{R})| = \frac{1}{e} \frac{d}{dR} V'(R). \quad (2.13)$$

$\vec{E}(\vec{R})$ is radially inward for $R > R_e$ and outward for $R < R_e$.

The resultant $m_l = 0$ adiabatic interatomic-potential-energy curves are obtained as before and are written

$$V_{2S}(R) = V'(R) - \epsilon(R) + \Delta - \frac{1}{2}i\gamma B^2(R), \quad (2.14a)$$

$$V_{2P}^0(R) = V'(R) + \epsilon(R) - \Delta - \frac{1}{2}i\gamma A^2(R), \quad (2.14b)$$

where ϵ , A , and B are defined as before, with \vec{E} now given by (2.13). Except at $R \approx 0$, $V'(R) \gg \epsilon(R)$, and the real parts of the optical potentials in Eqs. (2.14a) and (2.14b) are accurately approximated simply by V' . The magnitude of the $B^2(R)$ term in the opacity coefficient, obtained with the analytic Morse fit (2.11) in (2.13), is shown in Fig. 6 for $R \gtrsim a_0$. [The value of $B^2(R)$ for $R \lesssim a_0$ is unimportant due to the extremely repulsive character of $V'(R)$ for $R \lesssim a_0$; for the range of thermal velocities of interest, the atoms will not penetrate closer than

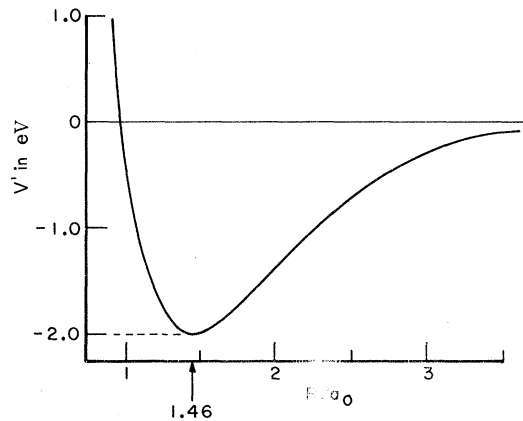


FIG. 5. $X^1\Sigma^+$ ground-state interatomic potential $V'(R)$ of $(\text{HeH})^+$.

a_0 .] The values of B^2 for $\mu^- \alpha$ are greatly reduced over comparable results for $\mu^- p$ in spite of the fact that electric field strengths are about the same in both cases, namely of order e/a_0^2 . This arises because of the much larger Lamb shift for $\mu^- \alpha$ and because its nuclear charge is 2. There is a very slight bump in $B^2(R)$ for $R \geq R_e$, which is not evident on the scale of Fig. 6. This bump accounts for only a small fraction of the quenching. Most quenching occurs in the region $a_0 \lesssim R \lesssim R_e$, and particularly near $R \approx a_0$, where $B^2(R)$ is increasing rapidly. The values of B^2 (which depend on the derivative of V') and hence, also the cross-section results, are found to be extremely sensitive to the precise form of V' in this region.

With reference to the applicability of the Hellmann-Feynman theorem in the present case, which leads to Eq. (2.13), we note that although the electronic wave function used in Ref. 17 is not exact, it does not contain R explicitly, but only through a set of variational parameters which are varied to minimize the energy. Under these circumstances,¹⁸ the theorem still applies although the electric fields obtained from Eq. (2.13) may still be subject to gross inaccuracies. Since the energy estimates of the ground state of $(\text{HeH})^+$ are variational, the curve V' is good to second order in the errors of the wave function, but this property does not apply to the electric field \vec{E} .

III. ADIABATIC APPROXIMATION

For the relative kinetic energies below threshold that we are interested in, we will assume that both collisions, $\mu^- p(2S)$ on H and $\mu^- \alpha(2S)$ on He, evolve adiabatically along the slightly complex optical potentials $\mathcal{U}_{2S}(R)$, that is, we assume one-channel processes throughout. In a time-dependent view, nonadiabatic excitation processes to the adiabatic Ψ_{2P}^0 state [as well as to the excited channels that connect adiabatically to the $2P(m_l = \pm 1)$ states] are neglected as intermediate states. No permanent excitation outside the collision region can occur at these energies below threshold. In this calculational approach quenching occurs since the adiabatic state Ψ_{2S} contains a component of the decaying $2P$ state during a collision.

A simple criterion to judge the validity of the adiabatic approximation requires that

$$\Delta E \tau_c > \hbar, \quad (3.1)$$

where ΔE is the energy separation of the adiabatic states and τ_c is the collision time. For $\mu^- p$, if we very roughly set ΔE equal to its asymptotic value 2Δ , and $\tau_c = R_c/v_0$, where the interaction range $R_c \sim 1a_0$ and v_0 is the incident relative velocity of $\mu^- p$ with respect to the nucleus of H, then inequality

(3.1) is satisfied for incident relative velocities v_0 up to approximately the threshold value; at thermal velocity (3×10^5 cm/sec), $\Delta E \tau_c > 5\hbar$. More precisely, criterion (3.1) should be evaluated at all R ,

$$\int_0^\infty \frac{\Delta E(R)}{v(R)} dR > \hbar. \quad (3.2)$$

Since the real part of the adiabatic curve $\mathcal{U}_{2S}(R)$ for $\mu^- p$ is everywhere attractive, the velocity $v(R)$ increases monotonically as R decreases. However ΔE also increases monotonically. Further, there are no near-crossing regions where nonadiabatic effects might be particularly important. The net effect of (3.2) is not appreciably different from the crude asymptotic estimates.

For $\mu^- \alpha$ this adiabatic criterion is much better satisfied. The Lamb shift for $\mu^- \alpha$ is about 1.4 eV, velocities are definitely in the thermal range, and the interaction region is somewhat larger than a_0 , which leads to $\Delta E \tau_c \approx 20\hbar$. We have not discussed excited states of $(\text{HeH})^+$. The energy separation between the ground $X^1\Sigma^+$ state of $(\text{HeH})^+$ and the first excited $^1\Sigma^+$ state, which asymptotically goes to $\text{He}^+ + \text{H}$ and which is everywhere repulsive, is much larger than the energy separation of the $2S$ and $2P$ adiabatic states associated with the ground $X^1\Sigma^+$ electronic state.

As a final point, it is perhaps useful to consider the case of close collisions where the interaction potential may actually be momentarily large, and both adiabatic channels are equally populated. Here, both channels will contain equal $2S$ and $2P$ components and hence will be equally attenuated. We suggest that even this extreme case where both channels are equally populated and equally attenuated is in fact not unlike the adiabatic approach where decay occurs solely from the lower channel.

IV. QUANTUM-MECHANICAL PARTIAL-WAVE CALCULATION

A quantum-mechanical treatment of the relative interatomic motion is desirable, particularly for $\mu^- p$ on H, because of the small values of the angular momentum. We can roughly estimate classi-

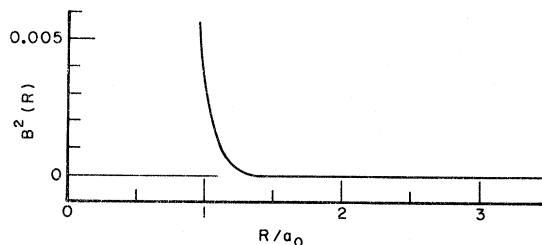


FIG. 6. $B^2(R)$ vs R for $(\mu^- \alpha)^+$ on He.

cally this maximum value of the angular momentum that is expected to be important. For μ^-p the reduced mass of the relative motion of μ^-p on H given by $M_K \equiv m_p(m_p + m_\mu)/(2m_p + m_\mu)$ is $967m_e$, and for the energies of interest the maximum impact parameter b is about a_0 . At a thermal velocity $v_0 = 3 \times 10^5$ cm/sec the angular momentum is then $bM_K v_0 \approx \hbar$. Even at a relative kinetic energy well above threshold of 1 eV, the angular momentum is only about $6\hbar$. For $\mu^- \alpha$, the relative mass is $3700m_e$ and the impact parameter is somewhat larger, which leads to somewhat higher values of the angular momentum.

Since the optical potentials are central and the values of the angular momentum are low, a partial-wave analysis is quite useful to obtain the absorption cross section, with only a limited number of partial waves expected to contribute. The absorption or quenching cross section for the l th partial wave is given as

$$\sigma_l = (\pi/K_0^2)(2l+1)(1 - |e^{2i\delta_l}|^2), \quad (4.1)$$

where $\hbar K_0 \equiv M_K v_0$ is the asymptotic wave number of the relative motion and $\delta_l(K_0)$ is the l th phase shift. $\delta_l(K_0)$ is now complex and is conveniently written in the form $\delta_l = \eta_l + i\frac{1}{2}\gamma\mu_l$, since the imaginary (Im) part of δ_l will be shown to be proportional to γ . (μ_l has inverse energy units.)

Evaluation of the phase shifts in the JWKB approximation leads¹⁹ to the following equation for $\text{Im}(\delta_l)$:

$$\begin{aligned} \text{Im}(\delta_l) &= \text{Im} \int_{R_{0,l}}^{\infty} K(R') dR' \\ &= \text{Im} \int_{R_{0,l}}^{\infty} \left\{ (2M_K/\hbar^2)[E_0 - V_{2s}(R') + i\frac{1}{2}\gamma P(R')] \right. \\ &\quad \left. - (l + \frac{1}{2})^2/R'^2 \right\}^{1/2} dR', \quad (4.2) \end{aligned}$$

where $P(R) = B^2(R)$, E_0 is the incident relative kinetic energy which is conserved since the scattering is elastic, $V_{2s}(R)$ represents the real parts of the optical potentials [Eq. (2.10a) for μ^-p and Eq. (2.14a) for $\mu^- \alpha$, respectively], $l(l+1)$ is replaced, as usual, by $(l + \frac{1}{2})^2$, and $R_{0,l}$ is the largest classical-turning-point solution of the motion, for angular momentum l of the equation

$$E_0 - V_{2s}(R) - \hbar^2(l + \frac{1}{2})^2/2M_K R^2 = 0. \quad (4.3)$$

The scattering phase shift δ_l is defined relative to the phase of a free particle, which then requires that in the calculation of the elastic-scattering phase shift an analogous phase integral for the free motion be subtracted off. However, for the calculation of the imaginary reactive phase shift there is clearly no analogous subtraction. Since the imaginary term in the optical potential is so small, it

suggests that one can approximately evaluate $\text{Im}(\delta_l)$ by simply expanding the integral functional about $\gamma=0$. The first nonvanishing imaginary term in the expansion leads to the following approximate expression for μ_l :

$$\begin{aligned} \mu_l(E_0) &\approx + \frac{M_K}{\hbar^2} \int_{R_{0,l}}^{\infty} P(R') \left/ \left(\frac{2M_K}{\hbar^2} [E_0 - V_{2s}(R')] \right. \right. \\ &\quad \left. \left. - \frac{(l + \frac{1}{2})^2}{R'^2} \right)^{1/2} dR' \right. \\ &= \frac{1}{\hbar} \int_{R_{0,l}}^{\infty} \frac{P(R')}{v_l(R')} dR', \quad (4.4) \end{aligned}$$

where $v_l(R)$ is the classical radial velocity and depends on the angular momentum l . The energy-level width $\frac{1}{2}\gamma$ will in general be small compared with $\mu_l(E)$ (except possibly at a special value of the energy discussed separately below), and hence one has approximately

$$1 - |e^{2i\delta_l}|^2 \approx 2\gamma\mu_l(E_0).$$

Since for both collisions the atoms involved are homonuclear, the over-all wave function must be made symmetric or antisymmetric with respect to interchange of the coordinates and spins of the two nuclei, depending on whether the nuclei are fermions or bosons. This added complexity gets translated into the partial-wave analysis by having the sums over the angular momentum l restricted to either even or odd values.²⁰ However, if more than a few partial waves contribute to the total cross section and their values do not vary abruptly for different l 's then to a good approximation one can still express the total quenching cross section by the usual result of potential scattering where exchange symmetry plays no role:

$$\begin{aligned} \sigma_S &\approx \frac{\pi}{K_0^2} \sum_l (2l+1)(1 - |e^{2i\delta_l}|^2), \\ &\approx (8\pi/K_0^2) \text{Im} \sum_l (l + \frac{1}{2})\delta_l \\ &= \frac{4\pi\gamma}{\hbar K_0^2} \sum_l (l + \frac{1}{2}) \int_{R_{0,l}}^{\infty} \frac{P(R')}{v_l(R')} dR'. \quad (4.5) \end{aligned}$$

Numerical integration of Eq. (4.4) for μ^-p on H was carried out for relative kinetic energies E_0 up to the threshold value (0.2 eV); the results for the partial cross sections are shown in Fig. 7. Even for $E_0 = 0.2$ eV only partial waves with $l \leq 5$ gave a non-negligible contribution and it was estimated that they provided over 95% of the total quenching cross section; for the energy range of interest the centrifugal barrier term excludes partial waves with $l > 5$ from the interaction region

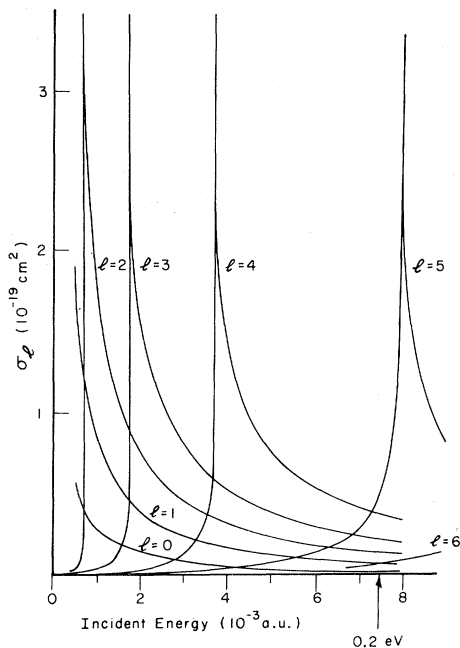


FIG. 7. Calculated partial quenching cross sections, σ_l , as a function of the incident relative kinetic energy for μ^-p on H.

where quenching occurs. The results for the total Stark-mixing quenching cross sections σ_s are shown in Fig. 8.

The sharp infinite peaks in each of the partial cross sections shown in Fig. 7 are of course unphysical and arise because of orbiting resonances.²¹ Consider the effective potential for the l th partial wave

$$V_l(R) = V_{2s}(R) + \hbar^2(l + \frac{1}{2})^2 / 2MR^2. \quad (4.6)$$

The form of this potential for $\mu^-p(2S)$ on H is given in Fig. 9 for various l ; if l is sufficiently large $V_l(R)$ will be monotonically repulsive as $R \rightarrow 0$. However for lower values of l , $V_l(R)$ has both a repulsive barrier and an attractive well. For energies E just below and then above the maximum in the repulsive bump, for a given value of l , there will be a discontinuous jump in the classical turning point resulting in an unphysical discontinuous change in the phase shift as calculated in the WKB approximation. The WKB approximation is not valid in this region since the classical radial velocity $v_l(R)$ approaches zero; because of the angular momentum there will be considerable orbiting about the center of force. The sharp orbiting resonances in Fig. 7 are infinite because of the approximate fashion in which the phase shifts are calculated using Eq. (4.4). Since the WKB approach is invalid in this region in any case it would not help to improve upon the approximation in Eq.

(4.4); one can simply, in a rough sense, smooth out the results by essentially neglecting the unphysical resonance peaks. The WKB approximation also does not account for the effects of possible quasibound states in the attractive well.

For $\mu^- \alpha$ on He, partial waves with l up to 16 contribute for kinetic energies in the thermal range; because of the increased relative mass, the centrifugal barrier term is not as effective in excluding higher partial waves from the interaction region. Results are again affected by the orbiting resonance problem. However, in this instance the resonances are extremely narrow, and in Fig. 10 we present results for the total quenching cross section as a function of the relative kinetic energy, where the resonances have been omitted. These results were obtained with the Morse-potential fit of Eq. (2.11) for V' . The dominant contribution to σ_s (generally greater than 90%) comes from the inner region, $R \lesssim R_e$, and particularly near $R \approx a_0$. For $\mu^- \alpha$, σ_s is quite sensitive to the precise form of V' in the region $R \approx a_0$ first because $B^2(R)$ is sensitive to V' , and second because the atoms spend a relatively long time at this separation since V' is repulsive. The potential, and even more so the electric field, is varying rapidly in this region. The form of V' for $R \gtrsim R_e$ also plays a role, since it sets the height of the corresponding effective potential for the l th partial wave, thereby determining the number of partial waves that can enter the quenching region. With relative-

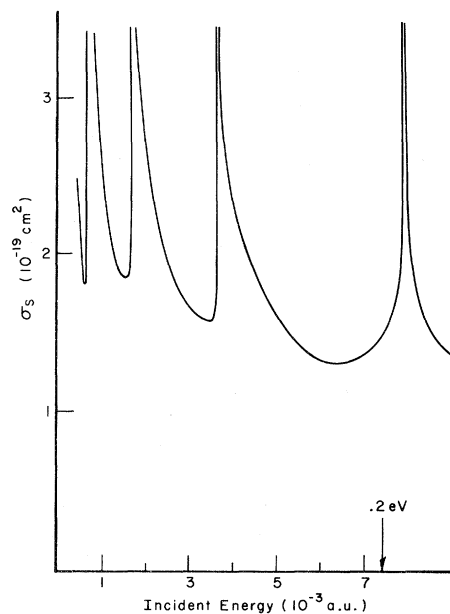


FIG. 8. Calculated total quenching cross section σ_s vs incident energy for μ^-p on H.

ly small changes in the fit to V' the results for σ_s are found to vary by as much as a factor of 3. In addition there are uncertainties in the numerically calculated values of $V'(R)$ ¹⁷ to which we fit the Morse potential.

Quenching at long range due to the van der Waals interaction has not been included. For μ^-p , the interatomic potential curve was estimated in lowest order with atomic orbitals and so has typical exponential fall off. In second order, but still neglecting couplings to different principal-quantum-number states of μ^-p the leading term in the interaction leads asymptotically to $c(R) = \lambda/R^3$, but since λ is proportional to the induced dipole moment of μ^-p which is so small we have neglected this long-range effect. Similarly, we have neglected van der Waals quenching of μ^-a .

Quenching due to an external Auger effect of the target electrons has also been neglected. Estimation of this effect¹⁰ for μ^-p in the Born approximation at 1 eV indicates that, at the thermal velocities of interest here, the associated cross section will be much smaller than the Stark-mixing cross section. We believe the same is true for μ^-a .¹⁰

Perturbative treatment of the interatomic interactions is invalid if the muonic systems directly approach the nucleus. The mutual nuclear repulsion prevents μ^-a from approaching closely the He nucleus at thermal velocities. For μ^-p however, the potential curve is attractive. At distances $R \sim a_\mu$ (Bohr radius of μ^-p) the perturbative approach is no longer valid, but we do not expect this breakdown to affect significantly our results for σ_s .

V. CLASSICAL PATH APPROACH

Although, as discussed in Sec. IV, a quantum-mechanical approach is clearly desirable because of the relatively few angular momentum terms that contribute to the collision for the velocities of

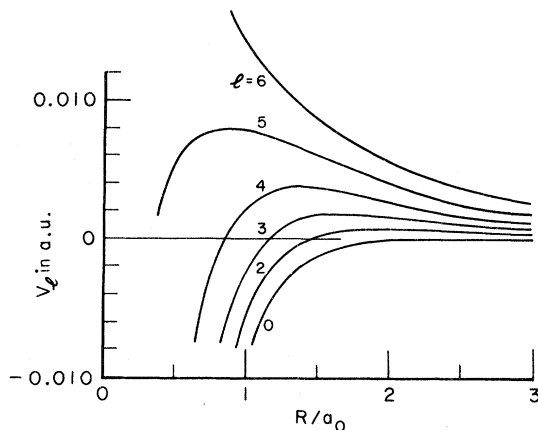


FIG. 9. Effective interatomic potential for the l th partial wave, $V_l(R)$, for μ^-p on H.

interest, we present here also, because of their calculational simplicity and as a check on the quantum calculations, time-dependent impact-parameter calculations of these cross sections. The atoms are here assumed to move along definite trajectories $\vec{R}(t)$ which will be specified later; the atoms become moving centers of force that subject the internal motion of muon and electron(s) to explicit time-dependent perturbation potentials, which will cause transitions among the internal states. As in Sec. IV we take the adiabatic limit, neglecting excitations of either the muonic or electronic states that may be caused by the time-dependent electrostatic potential or dynamic nonadiabatic couplings. Since the internal states are taken to be quantized along the interatomic \vec{R} axis, dynamic couplings will occur because of the radial and angular velocities of the axis relative to fixed axes during the collision. Relative velocities are so low that electronic and muonic translational factors play no role.

For μ^-p on H, the electronic 1S wave function has no dependence on \vec{R} , and therefore has no explicit dependence on time aside from the usual exponential time factor. We can then separate out the electronic motion, leading to an effective Schrödinger equation for the internal motion of μ^-p ,

$$i\hbar \frac{\partial}{\partial t} \chi(\vec{r}_\mu, t) = \{H_{\text{eff}}(\vec{r}_\mu; \vec{R}(t))\} \chi(\vec{r}_\mu, t). \quad (5.1)$$

We expand χ in terms of the time-dependent adiabatic basis states, $\Psi_{2S}^m[\vec{r}_\mu; \vec{R}(t)]$ and $\Psi_{2P}^m[\vec{r}_\mu; \vec{R}(t)]$ with corresponding energies $\epsilon_{2S}[\vec{R}(t)]$ and $\epsilon_{2P}^m[\vec{R}(t)]$, which represent lowest-order solutions and first-order corrected energies of the time-independent Schrödinger equation with the Hamiltonian $H_{\text{eff}}(\vec{r}_\mu; \vec{R})$, in which \vec{R} and hence t , appear only

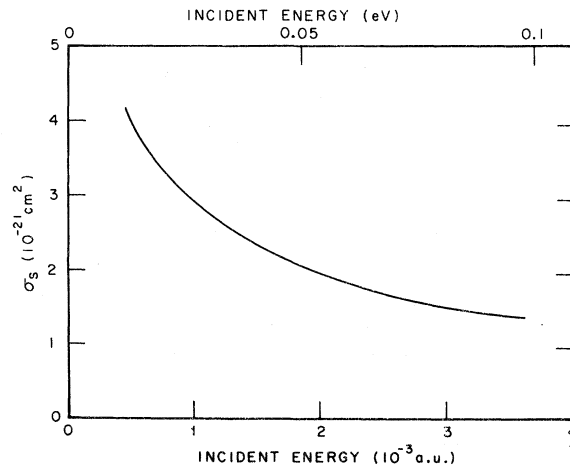


FIG. 10. Calculated total quenching cross section σ_s vs incident energy for $(\mu^-a)^+$ on He.

parametrically. χ is then written

$$\begin{aligned} \chi(\tilde{\mathbf{r}}_\mu, t) = & a_{2S}(t) \Psi_{2S}(\tilde{\mathbf{r}}_\mu; R) \exp \left[- \left(\frac{i}{\hbar} \right) \int_{-\infty}^t \epsilon_{2S}(t') dt' \right] \\ & + \sum_{m_l = -1, 0, 1} a_{2P}^{m_l}(t) \Psi_{2P}^{m_l}(\tilde{\mathbf{r}}_\mu; R) \\ & \times \exp \left[- \left(\frac{i}{\hbar} \right) \int_{-\infty}^t \epsilon_{2P}^{m_l}(t') dt' \right], \quad (5.2) \end{aligned}$$

where the amplitudes are now complex. The adiabatic solutions are orthonormal for any R .

Upon substitution of Eq. (5.2) in the Schrödinger equation (5.1), it is straightforward to obtain the coupled equations which the amplitudes satisfy, and a general expression for the total depletion rate of the state χ due to radiative decay from the $2P$ components, with inclusion of all the nonadiabatic coupling terms. In the adiabatic limit these couplings are dropped, and the only remaining coupling between the adiabatic states is that due to H_{decay} , which is treated in lowest order. This leads to the following approximate expression for the amplitude a_{2S} , which at $t = -\infty$ has the value $a_{2S}(-\infty) = 1$,

$$a_{2S} \simeq 1 - \frac{\gamma}{2\hbar} \int_{-\infty}^t B^2(t') dt'. \quad (5.3)$$

For specified values of the relative kinetic energy and impact parameter, the depletion rate of the asymptotic $2S$ state is

$$\mathcal{R} \simeq \frac{d}{dt} (|a_{2S}|^2) \simeq (-\gamma/\hbar) B^2(t) |a_{2S}(t)|^2,$$

and the corresponding total quenching is

$$1 - |a_{2S}(\infty)|^2 \simeq \frac{\gamma}{\hbar} \int_{-\infty}^{\infty} B^2(t') dt'. \quad (5.4)$$

The total quenching cross section, involving integration of (5.4) over all impact parameters b is

$$\begin{aligned} \sigma_s^{\text{I.P.}} & \equiv \int_0^{\infty} 2\pi b db (1 - |a_1(\infty)|^2) \\ & = \frac{\gamma}{\hbar} \int_0^{\infty} db \int_{-\infty}^{\infty} dt 2\pi b B^2(R(t)). \quad (5.5) \end{aligned}$$

Since the interatomic potential is so weak for μ^-p on H we assume a straight-line trajectory $\tilde{\mathbf{R}}(t) = b\hat{i} + z\hat{k}$, where \hat{i} and \hat{k} are unit vectors perpendicular and along the initial direction of motion and where $z = v_0 t$. Then since $dt = dz/v_0$, Eq. (5.5) can be expressed as

$$\begin{aligned} \sigma_s^{\text{I.P.}} & = \frac{\gamma}{\hbar v_0} \int_0^{\infty} db \int_{-\infty}^{\infty} dz 2\pi b B^2(R) \\ & = \frac{4\pi\gamma}{\hbar v_0} \int_0^{\infty} dR R^2 B^2(R). \quad (5.6) \end{aligned}$$

Substitution for $B^2(R)$ from (2.8) in (5.6) and evaluation of the integral leads to

$$\sigma_s^{\text{I.P.}} = 0.39(\pi a_0^2)(a_0\gamma/\hbar v_0),$$

which at typical thermal energies ($\frac{1}{40}$ eV) leads to a value for the cross section of 3.7×10^{-19} cm².

For collisions of μ^- on He, an analogous approach is used. Now however, the electronic wave function of $(\text{HeH})^+$ depends on R , and its partial time derivatives will not vanish, but since the wave function is assumed normalized and we exclude excited electronic states the equations satisfied by the amplitudes in the expansion of the muonic wave function are unaffected. In particular Eq. (5.5) remains valid, where the electric fields $\bar{\mathbf{E}}$ used in $B^2(R)$ are those obtained from V' .

The potential for the relative motion, which is approximated by $V'(R)$ is in this case strong enough so that at these low values of the relative velocity it is appropriate to use the classical path approximation. This is particularly important since the opacity or absorptive coefficient $P(R) = B^2(R)$ is strongly dependent on R near the origin and hence it is essential to have well defined the distance of closest approach R_c (classical turning point). The linear path would lead to too large cross sections because of the oversampling of small distances. Also because of the repulsive character of the potential for small R , the classical path will accurately reflect the time spent in the vicinity of the turning point where the absorption will be greatest.

The classical elastic scattering solution for given energy E_0 and impact parameter b , is symmetric about the distance of closest approach $R_c(b)$ defined by the largest zero of

$$E_0 - V'(R) - (E_0 b^2)/R^2 = 0;$$

noting that $dt = dR/v_b(R)$, where v_b is the magnitude of the velocity for particular b . Since the initial state of the He atom is spherically symmetric, the quenching cross section can be written

$$\sigma_s^{\text{I.P.}} = \frac{2\gamma}{\hbar} \int_0^{\infty} 2\pi b db \int_{R_c(b)}^{\infty} \frac{B^2(R)}{v_b(R)} dR. \quad (5.7)$$

Finally, since the classical angular momentum is just $\hbar l = M_K v_0 b$, where M_K is again the relative mass, $\sigma_s^{\text{I.P.}}$ can be written

$$\sigma_s^{\text{I.P.}} = \frac{4\pi\gamma}{\hbar K_0^2} \int_0^{\infty} l dl \int_{R_c(l)}^{\infty} \frac{B^2(R)}{v_l(R)} dR,$$

where $\hbar K_0 = M_K v_0$ is the initial wave number. This result is analogous to the quantum WKB expression (4.5), except that the sum over discrete l is replaced by an integral over continuous l . Upon evaluation of the integral using the Morse-potential

fit for V' , we obtain results similar to the quantum-mechanical estimates. At thermal velocity, the value of the cross section is 1.1×10^{-20} cm².

VI. DISCUSSION AND COMPARISON WITH EXPERIMENT

For both collision systems under consideration, the results of the impact-parameter calculations described in Sec. V are in reasonably close agreement with the quantum-mechanical estimates over the range of collision energies studied. It should be noted, however, that for collisions of $\mu^- \alpha$ on He, a straight-line path is not at all adequate, leading to results that are nearly an order of magnitude too large at the lower collision energies compared with the quantum-mechanical results. Other than the Stark quenching collision process [$\mu^- p(2S) + H \rightarrow \mu^- p(1S) + \gamma + H$] which we calculate, the only other two-body collision process that is allowed energetically is the external Auger process [$\mu^- p(2S) + H \rightarrow \mu^- p(1S) + H^+ + e^-$]. Previous calculations¹⁰ indicate that the external Auger process is unimportant. The same conclusion applies for $\mu^- \alpha(2S)$ quenching.

A calculation has recently been done²² on the quenching of $\mu^- \alpha(2S)$ in helium gas in which the dominant quenching occurs through formation of the bound molecule $(\mu^- \alpha)^+ \text{He}$ and subsequent electromagnetic transition to the ground 1S state. The calculated quenching rate is comparable to our theoretical results for $\mu^- \alpha(2S)$ and about one order of magnitude greater than the observed quenching rate. This quenching process requires the forma-

tion of the bound molecule and hence differs from the Stark quenching process we have calculated in this paper.

We can make a comparison of the theoretical results for quenching of $\mu^- \alpha$ with available experimental results. From observations of the metastable 2S state of $\mu^- \alpha$ in He at different pressures⁴ a value of the total quenching cross section has been obtained, which is in the nature of an upper bound; the result is about 10^{-22} cm². For thermal kinetic energy of $\mu^- \alpha$ the theoretical value of σ_s is 3×10^{-21} cm² (Fig. 10) which is larger by about an order of magnitude than this experimental value. We feel, as noted previously, that uncertainties in the precise form of the interatomic potential $V'(R)$ at small separations is responsible for the discrepancy. This points to the need for a more precise determination of V' .

At present there is no experimental information about the quenching cross section σ_s for $\mu^- p(2S)$, and indeed no direct information on the formation of $\mu^- p(2S)$.²³ An experiment is planned²⁴ to search for the formation of $\mu^- p(2S)$ in H₂ gas and to measure the quenching cross section through observation of delayed 2P-1S x rays as a function of H₂ gas pressure. The small theoretical value of σ_s for $\mu^- p(2S)$ below the 2S-2P inelastic threshold implies that if there is sufficient formation of $\mu^- p(2S)$ with energies below this threshold, then fine-structure and hyperfine-structure measurements might be done on $\mu^- p$ in the $n=2$ state, analogous to that on $\mu^- \alpha$ in the $n=2$ state.⁵

*Research supported in part by the Air Force Office of Scientific Research, AFSC, under AFOSR Contract No. F44620-70-C-0091 and the National Science Foundation under Contract No. GP 27714.

†Deceased 30 June 1971.

¹A. Di Giacomo, Nucl. Phys. B **11**, 411 (1969); B **23**, 641 (1970); E. Campani, Nuovo Cimento Lett. **4**, 512 (1970).

²V. W. Hughes, *Atomic Physics 3*, edited by S. J. Smith and G. K. Walters (Plenum, New York, 1973), p. 1.

³C. S. Wu, *Atomic Physics 3*, edited by S. J. Smith and G. K. Walters (Plenum, New York, 1973), p. 93.

⁴A. Placci, E. Polacco, E. Zavattini, K. Ziock, G. Carboni, U. Gastaldi, G. Gorini, G. Neri, and G. Torelli, Nuovo Cimento A **1**, 445 (1971); G. Carboni, A. Placci, E. Zavattini, U. Gastaldi, G. Gorini, O. Pitzurra, G. Neri, E. Polacco, G. Torelli, J. Duclos, J. Picard, and A. Vitale, Nuovo Cimento Lett. **6**, 233 (1973).

⁵E. Zavattini, Fourth International Conference on Atomic Physics, July, 1974, Heidelberg, Germany (to be published).

⁶E. Campani, Nuovo Cimento Lett. **4**, 982 (1970).

⁷L. Spitzer, Jr. and J. L. Greenstein, *Astrophys. J.*

114, 407 (1951); J. Shapiro and G. Breit, *Phys. Rev.* **113**, 179 (1959).

⁸A. S. Wightman, *Phys. Rev.* **77**, 521 (1950); A. S. Wightman, Ph.D. thesis (Princeton University, 1949) (unpublished).

⁹T. B. Day, G. A. Snow, and J. Sucher, *Phys. Rev. Lett.* **3**, 61 (1959) and *Phys. Rev.* **118**, 864 (1960).

¹⁰M. Leon and H. A. Bethe, *Phys. Rev.* **127**, 636 (1962).

¹¹M. Leon, *Phys. Lett. B* **35**, 413 (1971).

¹²A. Alberigi Quaranta, A. Bertin, G. Matone, F. Palmonari, A. Placci, P. Dalpiaz, G. Torelli, and E. Zavattini, *Nuovo Cimento* **47**, 72 (1967).

¹³Radiative decay rates of $\mu^- p$ and $\mu^- \alpha$ are those of a hydrogenic system scaled in terms of their respective reduced masses and nuclear charges. See, e.g., H. A. Bethe and E. E. Salpeter, *Quantum Mechanics of One- and Two-Electron Atoms* (Springer-Verlag, Berlin, 1957), Sec. 63.

¹⁴G. Kodosky and M. Leon, *Nuovo Cimento B* **1**, 41 (1971).

¹⁵From kinetic theory, the depletion rate at a particular velocity is equal to $n v \sigma$, where n is the density of target atoms, v is the velocity of $\mu^- p$, and σ is the quench-

ing cross section at that value of velocity.

- ¹⁶V. W. Hughes, H. Rosenthal, and C. S. Wu, *Bull. Am. Phys. Soc.* **16**, 617 (1971); K. N. Huang *et al.*, *High-Energy Physics and Nuclear Structure*, edited by G. Tibell (North-Holland, Amsterdam, 1974), p. 312.
- ¹⁷L. Wolniewicz, *J. Chem. Phys.* **43**, 1087 (1965), and references therein.
- ¹⁸J. O. Hirschfelder and W. J. Meath, *Intermolecular Forces*, edited by J. O. Hirschfelder (Interscience, New York, 1967), p. 53.
- ¹⁹The quasiclassical approximation is discussed, e.g., in L. D. Landau and E. M. Lifshitz, *Quantum Mechanics—Nonrelativistic Theory*, 2nd Ed. (Pergamon, New York, 1965), Sec. 126.
- ²⁰See, for example, S. Geltman, *Topics in Atomic Collision Theory* (Academic, New York, 1969), p. 183.
- ²¹N. F. Mott and H. S. W. Massey, *The Theory of Atomic Collisions*, 3rd Ed. (Oxford, New York, 1965).
- ²²G. Carboni and O. Pitzurra, Radiative Collisional Quenching of the Metastable Muonic Helium Ion $\mu\text{He}^+(2S)$ (unpublished). Preprint of April, 1974.
- ²³A. Placci *et al.*, *Phys. Lett.* **32B**, 413 (1970).
- ²⁴P. Egan *et al.*, Nevis proposal 5b, Columbia University (1971) and LAMPF proposal 206, Los Alamos Scientific Laboratory (1974).